RIP1 kinase mediates angiogenesis by modulating macrophages in experimental neovascularization

Takashi Ueta[a,b], Kenji Ishihara[a], Shoji Notomi[a], Jong-Jer Lee[a,c], Daniel E. Maidana[a], Nikolaos E. Efstathiou[a], Yusuke Murakami[d], Eiichi Hasegawa[a], Kunihiro Azuma[b], Tetsuya Toyono[b], Eleftherios I. Paschalis[e], Makoto Aihara[b], Joan W. Miller[a], and Demetrios G. Vavvas (Δημήτριος Γ. Βάββας)[a,1]

[a]Angiogenesis Laboratory, Department of Ophthalmology, Massachusetts Eye and Ear, Harvard Medical School, Boston, MA 02114; [b]Department of Ophthalmology, Graduate School of Medicine and Faculty of Medicine, The University of Tokyo, 113-8655 Tokyo, Japan; [c]Department of Ophthalmology, Kaohsiung Chang Gung Memorial Hospital, 833 Kaohsiung, Taiwan; [d]Department of Ophthalmology, Graduate School of Medical Science, Kyushu University, 812-8582 Fukuoka, Japan; and [e]Schepens Eye Research Institute, Massachusetts Eye and Ear, Harvard Medical School, Boston, MA 02114

Edited by Akrit Sodhi, Johns Hopkins University School of Medicine, Baltimore, MD, and accepted by Editorial Board Member Jeremy Nathans October 7, 2019 (received for review May 23, 2019)

Inflammation plays an important role in pathological angiogenesis. Receptor-interacting protein 1 (RIP1) is highly expressed in inflammatory cells and is known to play an important role in the regulation of apoptosis, necroptosis, and inflammation; however, a comprehensive description of its role in angiogenesis remains elusive. Here, we show that RIP1 is abundantly expressed in infiltrating macrophages during angiogenesis, and genetic or pharmacological inhibition of RIP1 kinase activity using kinase-inactive $RIP1^{K45A/K45A}$ mice or necrostatin-1 attenuates angiogenesis in laser-induced choroidal neovascularization, Matrigel plug angiogenesis, and alkali injury-induced corneal neovascularization in mice. The inhibitory effect on angiogenesis is mediated by caspase activation through a kinase-independent function of RIP1 and RIP3. Mechanistically, infiltrating macrophages are the key target of RIP1 kinase inhibition to attenuate pathological angiogenesis. Inhibition of RIP1 kinase activity is associated with caspase activation in infiltrating macrophages and decreased expression of proangiogenic M2-like markers but not M1-like markers. Similarly, in vitro, catalytic inhibition of RIP1 down-regulates the expression of M2-like markers in interleukin-4–activated bone marrow-derived macrophages, and this effect is blocked by simultaneous caspase inhibition. Collectively, these results demonstrate a nonnecrotic function of RIP1 kinase activity and suggest that RIP1-mediated modulation of macrophage activation may be a therapeutic target of pathological angiogenesis.

RIPK | necrosis | immune | neovascular | AMD

Pathological angiogenesis has been implicated in many disorders, including neovascular age-related macular degeneration (AMD), the leading cause of blindness in elderly individuals worldwide (1). During pathological angiogenesis, the abundant infiltration of macrophages supports vascular endothelial sprouting. Tissue-infiltrating macrophages are polarized into functional phenotypes, including classically activated (proinflammatory M1) and alternatively activated (antiinflammatory and tissue-remodeling M2) macrophages. Macrophages can undergo dynamic transitions between different functional states, potentially driven by the tissue microenvironment that dictates a transcriptional response (2). In angiogenesis, the importance of M2-like macrophages or the M1-to-M2 transition of phenotypes has been well-established through several angiogenesis models (3–8), including laser-induced choroidal neovascularization (CNV), a major mouse model of neovascular AMD (3, 5, 6, 8). However, current knowledge about the regulation of macrophage phenotypes and functions remains incomplete.

Previous studies have suggested a causative role for death receptors (9–13) and Toll-like receptors (14–16) in angiogenesis, including neovascular AMD (10, 13) and the well-established model of laser-induced CNV in mice (11, 16), although to date a consensus has not been reached (17, 18). Receptor-interacting protein 1 (RIP1) is an intracellular adaptor protein that relays signals from these receptors to regulate inflammation, apoptosis, and necroptosis (19–22). RIP1 is subjected to posttranslational modifications, including ubiquitination, phosphorylation of the kinase domains, and oligomerization via interaction with the RIP homotypic interaction motif (RHIM). Ubiquitinated RIP1 induces nuclear factor-kappa B (NF-κB)-mediated inflammation and cell survival, whereas deubiquitinated RIP1 forms a "ripoptosome" with caspase-8, cellular FLICE (FADD-like interleukin-1β-converting enzyme)-inhibitory protein, and the Fas-associated death domain (FADD), leading to either apoptosis or necroptosis (19). Phosphorylated and RHIM-oligomerized RIP1 exerts catalytic kinase activity to form a "necrosome" with RIP3 and mixed-lineage kinase-like protein, leading to necroptosis and inflammation (19, 20, 22). Because caspase-8 cleaves RIP1 to inhibit the necroptotic pathway, apoptosis is frequently induced as the primary mode of cell death, whereas necroptosis can be facilitated when the activity of caspase-8 or other apoptotic factors, including FADD, is down-regulated. Although kinase-dependent functions of RIP1 are usually pronecrotic, kinase-independent functions of RIP1 could be important for preventing the inappropriate activation of caspase-8–dependent apoptosis and RIP3-dependent necroptosis (23–26). The functions of RIP1 depend on cell types and the biological context,

Significance

Pathological angiogenesis has been implicated in diverse pathologies. Infiltrating macrophages, especially those activated to M2-like phenotype, are critically important for angiogenesis. Although the role of RIP1 kinase in the regulation of apoptosis, necroptosis, and inflammation has been well-established, its role in angiogenesis remains elusive, despite being abundantly expressed in angiogenesis-related infiltrating macrophages. This study demonstrates that RIP1 kinase inhibition attenuates angiogenesis in multiple mouse models of pathological angiogenesis in vivo and suggests a therapeutic role of RIP1 kinase inhibition in pathological angiogenesis. Mechanistically, the inhibitory effect on angiogenesis depends on RIP kinase inhibition-mediated caspase activation in infiltrating macrophages through suppression of M2-like polarization, and subsequent attenuation of pathological angiogenesis.

Author contributions: T.U. and D.G.V. designed research; T.U., K.I., S.N., J.-J.L., D.E.M., N.E.E., Y.M., E.H., K.A., T.T., and E.I.P. performed research; T.U. analyzed data; and T.U., K.I., Y.M., M.A., J.W.M., and D.G.V. wrote the paper.

The authors declare no competing interest.

This article is a PNAS Direct Submission. A.S. is a guest editor invited by the Editorial Board.

[1]To whom correspondence may be addressed. Email: demetrios_vavvas@meei.harvard.edu.

This article contains supporting information online at www.pnas.org/lookup/suppl/doi:10.1073/pnas.1908355116/-/DCSupplemental.

First published November 4, 2019.

and its role in angiogenesis remains largely unknown despite its relatively abundant expression in infiltrating macrophages.

In the present study, using genetically engineered mice and catalytic inhibitors for RIP1, RIP3, and caspases, we explored a pivotal nonnecrotic role of RIP1 in angiogenesis and macrophage polarization using in vivo and in vitro models of pathological angiogenesis.

Results

Inhibition of RIP1 Kinase Activity Suppresses CNV. To examine the role of RIP1 kinase activity in angiogenesis, we used a laser-induced CNV model, a well-established and one of the most commonly used angiogenesis models (27). In this model, we detect up-regulation of RIP kinases and caspases in retinal pigment epithelium (RPE)-choroid-sclera tissue containing CNV lesions during the phase of ongoing neovascular response with macrophage infiltration (Fig. 1*A* and *SI Appendix*, Fig. S1). Immunohistochemistry results also showed abundant expression of RIP1 protein in laser-induced CNV lesions in mice (Fig. 1*B*). Likewise, in human neovascular AMD, immunohistochemistry showed a relatively higher RIP1 protein expression in CD68-positive macrophages (Fig. 1*C*).

We next examined the effect of the catalytic inhibition of RIP1 on the development of laser-induced CNV using necrostatin-1 (Nec-1). Nec-1 was administered through intravitreal injections immediately after CNV induction. We observed a dose-dependent effect of Nec-1 that resulted in reduction of CNV lesion size (Fig. 2*A*). We also tested the effect of systemic administration of Nec-1. Alzet osmotic pumps loaded with dimethyl sulfoxide (DMSO) vehicle or Nec-1 were subcutaneously (s.c.) implanted the day before CNV induction. Seven days after CNV induction, Nec-1–treated mice showed significantly reduced CNV size compared with control mice (Fig. 2*B*), confirming that Nec-1 effects are independent of administration procedures. Moreover, to rule out the possibility that Nec-1's effect on CNV is due to its influence on acute cell death after laser application, Nec-1 was intravitreally injected on day 4, which also significantly reduced CNV size on day 7 (Fig. 2*C*). The longer-term effect of RIP1 kinase inhibition on CNV size

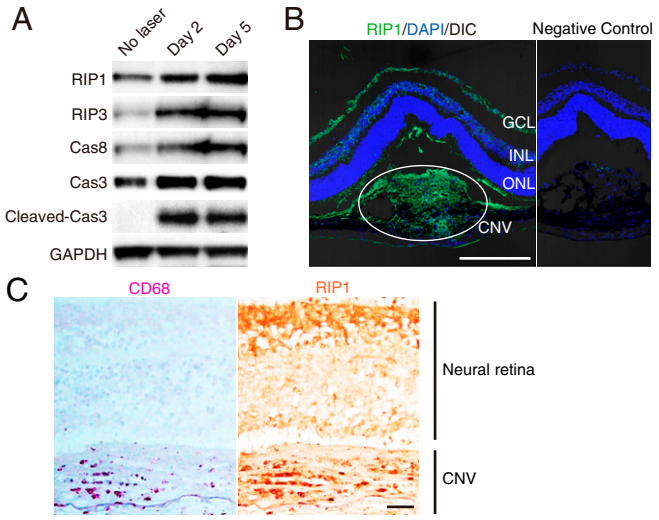

Fig. 1. RIP1 expression in CNV. (*A*) Western blot analysis of RIP and caspase pathways in RPE-choroid on days 0, 2, and 5 after CNV induction. (*B*) Immunohistochemistry of RIP1 in CNV on day 5 after induction by laser. (Scale bar, 100 μm.) DIC, differential interference contrast; GCL, ganglion cell layer; INL, inner nuclear layer; ONL, outer nuclear layer of the retina. (*C*) Immunohistochemistry of RIP1 and CD68 in human neovascular AMD. (Scale bar, 100 μm.)

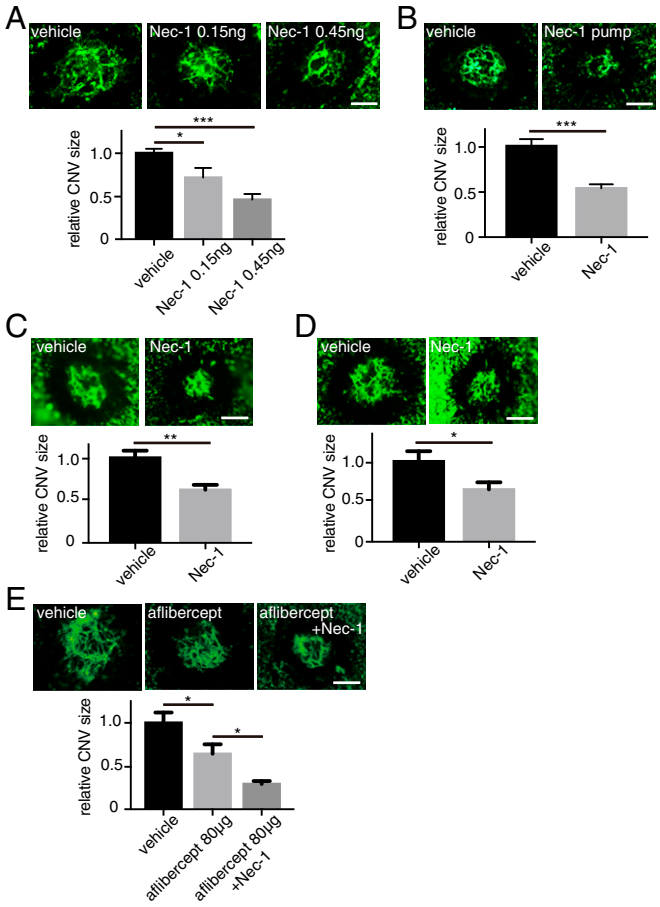

Fig. 2. Nec-1 attenuates angiogenesis in laser-induced CNV. (*A*) After CNV induction (day 0), DMSO vehicle or Nec-1 was intravitreally injected into the eyes of WT mice, and CNV size was assessed on RPE-choroidal flat mounts on day 7. $n = 10$ to 15 eyes per group. (*B*) DMSO vehicle or Nec-1 was administered through osmotic pumps that were s.c. implanted in WT mice the day before CNV induction. CNV size was assessed on RPE-choroidal flat mounts on day 7. $n = 6$ eyes per group. (*C*) DMSO vehicle or Nec-1 was intravitreally injected into the eyes of WT mice on day 4 and CNV size was assessed on day 7. $n = 10$ eyes per group. (*D*) DMSO vehicle or Nec-1 was intravitreally injected into the eyes of WT mice on day 3 and CNV size was assessed on day 14. $n = 10$ eyes per group. (*E*) DMSO vehicle or Nec-1 was intravitreally injected into the eyes of WT mice on day 0, PBS vehicle or aflibercept was intravitreally injected on day 4, and CNV size was assessed on day 7. $n = 10$ eyes per group. (Scale bars, 100 μm.) $^*P < 0.05$, $^{**}P < 0.01$, $^{***}P < 0.001$; Student's *t* test or 1-way ANOVA and post hoc Tukey's test. Data are mean ± SEM.

was determined by intravitreal injection of Nec-1 on day 0, which remained effective at least until day 14 (Fig. 2*D*). Lastly, we tested the effect of Nec-1 in conjunction with conventional antivascular endothelial growth factor (VEGF) therapy using aflibercept and demonstrated further reduction of CNV size compared with aflibercept treatment alone (Fig. 2*E*).

Caspase Activation Mediates the Effect of RIP1 Kinase Inhibition to Suppress CNV. To elucidate how the catalytic inhibition of RIP1 suppresses CNV, we first evaluated the involvement of RIP3 using RIP3-deficient mice and GSK′872, a catalytic inhibitor of RIP3. First, we observed that Nec-1 (RIP1 kinase inhibition) does not reduce CNV size in RIP3-deficient mice (Fig. 3*A*), indicating that RIP3 is necessary for Nec-1 to suppress CNV. Catalytic inhibition of RIP3 by GSK′872 decreased CNV size on day 7 in wild-type (WT) mice (Fig. 3*B*), whereas GSK′872 did not have an effect on RIP3-deficient mice (*SI Appendix*, Fig. S2*A*).

These results indicate that catalytic inhibition of RIP1 or RIP3 suppresses CNV, whereas complete loss of RIP3 protein does not (*SI Appendix*, Fig. S2*B*), suggesting a role for the RIP scaffold in angiogenesis inhibition when kinase activity is lost. We thus speculated that RIP kinase inhibition unmasks a kinase-independent RIP scaffold function that leads to CNV suppression.

Previous studies have shown that catalytic inhibition of RIP3 leads to caspase activation through the kinase-independent function of RIP1/RIP3 via the ripoptosome-like complex comprising RIP1, RIP3, caspase-8, and FADD (28, 29). It has also been shown that RIP1 kinase inhibition by Nec-1 treatment can induce caspase activation and apoptosis (30, 31). Consistent with these studies, RIP1 kinase inhibition led to caspase-3 activation in CNV lesions, which was abrogated by a pan-caspase inhibitor, Z-VAD-FMK (carbobenzoxy-valyl-alanyl-aspartyl-[*O*-methyl]-fluoromethylketone; Z-VAD) (Fig. 3*C*). In contrast, Nec-1 and/or Z-VAD treatment did not alter caspase-3 activation in eyes without CNV lesions (*SI Appendix*, Fig. S3). In addition, we directly assessed the formation of a ripoptosome-like complex in RPE-choroid tissues with CNV lesions (in conditions that prevent ripoptosome consumption). We observed that Nec-1 treatment up-regulated the association of RIP1, RIP3, and FADD, with caspase-8 (Fig. 3*D*).

This activation of caspases by RIP1 kinase inhibition appears to be important for CNV suppression. Indeed, caspase inhibition by Z-VAD abolished the inhibitory effect on CNV by Nec-1 (Fig. 3*E*). We further studied the effects of Nec-1 and Z-VAD on CNV by using fluorescein angiography (FA) to evaluate CNV leakage, and spectral domain optical coherent tomography (SD-OCT) to evaluate CNV size/thickness, as more clinically relevant modalities of CNV assessment. FA revealed that the severity of vascular leakage from CNV lesions decreased significantly with Nec-1 administration, and that this effect was abolished by the

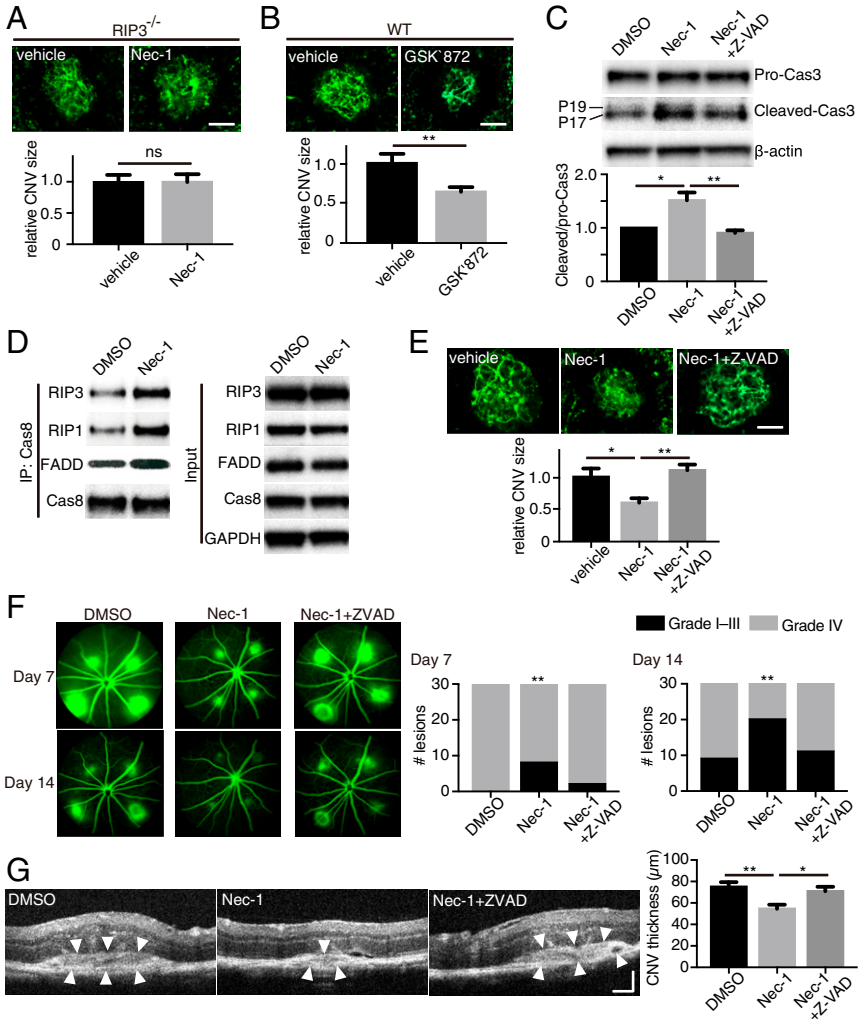

Fig. 3. Caspase activation mediates the attenuation of CNV by catalytic inhibition of RIP1. (*A*) CNV size on flat mounts on day 7 in RIP3$^{-/-}$ mice intravitreally injected with DMSO vehicle or Nec-1. $n = 8$ eyes per group. (Scale bar, 100 μm.) (*B*) CNV size on flat mounts on day 7 in WT mice intravitreally injected with DMSO vehicle or GSK′872, an inhibitor of RIP3 kinase activity. $n = 12$ eyes per group. (Scale bar, 100 μm.) (*C*) Western blot analysis of procaspase-3 and cleaved caspase-3 in RPE-choroid on day 5 after CNV induction and intravitreal injections with DMSO vehicle, Nec-1, or Nec-1+Z-VAD. $n = 3$ samples per group. (*D*) Western blots of caspase 8-containing ripoptosome-like complex immunoprecipitated from RPE-choroid 4 d after CNV induction and intravitreal injections with DMSO vehicle or Nec-1. Both groups equally received Z-VAD intravitreal injections to block the consumption of the formed ripoptosome-like complex. (*E*) CNV size on flat mounts on day 7 in WT mice intravitreally injected with DMSO vehicle, Nec-1, or Nec-1+Z-VAD. $n = 8$ eyes per group. (Scale bar, 100 μm.) (*F*) Fluorescein leakage from CNV lesions in WT mice was assessed on days 7 and 14 after CNV induction and intravitreal injections with DMSO vehicle, Nec-1, or Nec-1+Z-VAD. $n = 30$ lesions per group. (*G*) CNV thickness was assessed on cross-sectional images of CNV obtained through SD-OCT in WT mice on day 7 after CNV induction and intravitreal injections with DMSO vehicle, Nec-1, or Nec-1+Z-VAD. $n = 14$ lesions per group. (Scale bar, 100 μm.) *$P < 0.05$, **$P < 0.01$; ns, no significant difference; Student's *t* test or 1-way ANOVA and post hoc Tukey's test. Data are mean ± SEM.

pan-caspase inhibitor Z-VAD (Fig. 3*F*), indicating that Nec-1–induced suppression of angiogenesis is mediated through caspase activation. Similarly, CNV thickness in situ was also decreased by Nec-1, an effect that can be reversed through simultaneous injection of Z-VAD with Nec-1 (Fig. 3*G*). Based on these results, we infer that catalytic inhibition of RIP1 kinase activates caspases to attenuate CNV development.

RIP1 Kinase Inhibition Suppresses Angiogenesis through Caspase Activation in Multiple Models in Vivo. To address whether RIP1 kinase inhibitory effect on laser CNV can be reproduced in other angiogenesis models, we used an in vivo Matrigel plug assay. Using basic fibroblast growth factor (bFGF), which is commonly used to induce angiogenesis in Matrigel plugs, we evaluated RIP1 expression in the plugs via immunohistochemistry. We observed higher levels of RIP1 protein in F4/80(+) macrophages, whereas relatively low levels of RIP1 protein were found in CD31(+) vascular endothelial cells (*SI Appendix*, Fig. S4*A*). Administration of Nec-1 in the Matrigel decreased bFGF-induced angiogenesis as assessed by macroscopic color assessment (*SI Appendix*, Fig. S4*B*), hematoxylin and eosin staining (*SI Appendix*, Fig. S4*C*), and hemoglobin content (*SI Appendix*, Fig. S4*D*). Angiogenesis suppression by Nec-1 was abolished by the pan-caspase inhibitor Z-VAD (*SI Appendix*, Fig. S4 *B–D*). In addition to bFGF-induced angiogenesis, we also examined the effect of RIP1 kinase inhibition on tumor necrosis factor (TNF)-related apoptosis-inducing ligand (TRAIL)-induced angiogenesis (32). Again, angiogenesis was significantly suppressed by Nec-1, an effect that was abolished by Z-VAD (*SI Appendix*, Fig. S4 *E–G*).

As a clinically relevant ocular angiogenesis model, the alkali injury-induced corneal neovascularization model was used (33, 34). Alkali injury is an ocular emergency that can lead to severe ocular surface damage (35–37). Despite immediate irrigation followed by medical/surgical interventions, a significant number of patients suffer from deteriorating visual function because of loss of corneal transparency through neovascularization (34, 38, 39). In this model, we confirmed that RIP1 kinase inhibition by subconjunctival injections of Nec-1 ameliorated corneal neovascularization evaluated 10 d after injury, and the therapeutic effect was abrogated by concomitant Z-VAD injections with Nec-1 (*SI Appendix*, Fig. S5).

Taken together, these results suggest that RIP1 kinase inhibition by Nec-1 suppresses angiogenesis through caspase activation in multiple models of angiogenesis.

Infiltrating Macrophages Are the Main Target for Catalytic Inhibition of RIP1 to Suppress Angiogenesis. As our data suggest that RIP1 kinase inhibition results in caspase activation, we sought to identify if this leads to an increase in the terminal deoxynucleotidyl transferase dUTP nick-end labeling [TUNEL(+)] of cells. In treatment-naïve CNV lesions, TUNEL(+) cells were most abundantly detected during days 4 to 5 (*SI Appendix*, Fig. S6), the phase of ongoing angiogenic response with abundant macrophage infiltration (27). Nec-1 administration led to an increase in TUNEL(+) cells, and this effect was abolished by Z-VAD (Fig. 4*A*). Consistently, an increased number of TUNEL(+) cells was also observed in CNV lesions of RIP1 kinase-inactive RIP1$^{K45A/K45A}$ mice (*SI Appendix*, Fig. S7*A*) (40). Use of coimmunolabeling revealed TUNEL(+) cells stained for the macrophage/microglial cell marker Iba1 (in cytoplasm) (*SI Appendix*, Fig. S7*B*) but not for the endothelial cell marker CD31 (*SI Appendix*, Fig. S7*C*). Based on these results, we speculated that Nec-1 treatment induced caspase activation specifically in macrophages. Indeed, on immunohistochemistry, cleaved caspase-3 was observed predominantly in F4/80(+) macrophages in CNV lesions after Nec-1 treatment (Fig. 4*B*). To rule out the possibility that the cleaved caspase-3 might be attributed to phagocytosis of apoptotic cells, macrophages were depleted using clodronate, which did not lead to a significant increase of cleaved caspase-3 in nonmacrophage

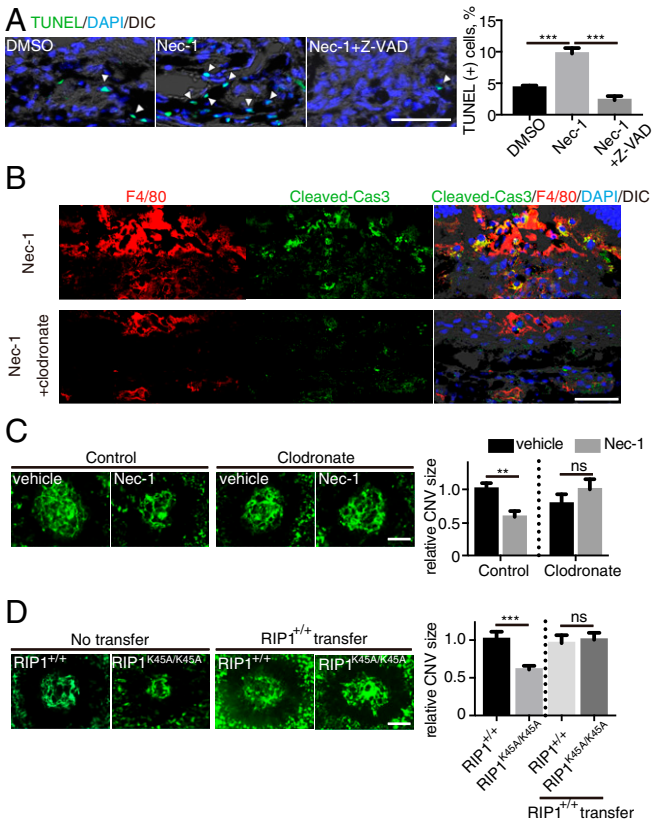

Fig. 4. Infiltrating macrophages are targets of catalytic inhibition of RIP1 to attenuate CNV. (*A*) TUNEL staining of CNV sections on day 5 after CNV induction and intravitreal injections with DMSO vehicle, Nec-1, or Nec-1+Z-VAD. $n = 6$ lesions per group. (Scale bar, 50 μm.) Arrowheads indicate TUNEL(+) cells. (*B*) Immunohistochemistry of day 4 CNV sections for cleaved caspase-3 and its localization in F4/80(+) macrophages after intravitreal injections (day 0) with Nec-1 and i.p. injections (day 2) with vehicle or clodronate. (Scale bar, 50 μm.) (*C*) CNV was induced in WT mice and DMSO vehicle or Nec-1 was intravitreally injected on day 0. The mice received i.p. injections with control or clodronate liposome on day 2. CNV size was assessed on flat mounts on day 7. $n = 8$ eyes per group. (Scale bar, 100 μm.) (*D*) CNV size on flat mounts on day 7 in RIP1$^{+/+}$ and RIP1$^{K45A/K45A}$ kinase-dead mice. The designated groups of mice received an adoptive transfer of bone marrow monocytes (5×10^6) from RIP1$^{+/+}$ mice on day 2. $n = 10$ eyes per group. (Scale bar, 100 μm.) $^{**}P < 0.01$, $^{***}P < 0.001$; ns, no significant difference; Student's *t* test or 1-way ANOVA and post hoc Tukey's test. Data are mean ± SEM.

cells (Fig. 4*B*), confirming that the immunolabeled cleaved caspase-3 was of macrophage origin.

The above results suggest that infiltrating macrophages may be the target for the catalytic inhibition of RIP1 to suppress angiogenesis. To further address this hypothesis, WT mice were divided into 2 groups: One group received intraperitoneal (i.p.) injections of clodronate liposomes at 2 d after CNV induction to deplete macrophages, and the other group received i.p. injections of control liposomes. Nec-1 did not suppress CNV development in mice with macrophage depletion, whereas it did suppress it in nondepleted mice (Fig. 4*C*). Furthermore, we used RIP1 kinase-inactive (RIP1$^{K45A/K45A}$) mice, and confirmed that genetic inhibition of RIP1 kinase activity reduces CNV size (Fig. 4*D*), as did pharmacological RIP1 kinase inhibition using Nec-1. To clarify the role of RIP1 kinase inhibition in macrophages, bone marrow monocytes of WT mice were adoptively transferred to the i.p. cavity of WT mice or RIP1$^{K45A/K45A}$ mice on day 2 after CNV induction (*SI Appendix*, Fig. S8). After the adoptive transfer, CNV size in RIP1$^{K45A/K45A}$ mice was significantly increased to a size similar to that in WT mice (Fig. 4*D*). Collectively, these data suggest

that catalytic inhibition of RIP1 suppresses angiogenesis, at least partially, by affecting the infiltrating macrophages.

Effects of RIP1 Kinase Inhibition on Macrophage Function. Although RIP1 kinase inhibition in macrophages and its effect on angiogenesis could be mediated by increased macrophage death and loss, it could also be a result of non–cell-death-mediated effects on macrophage function. Thus, to examine the latter, we investigated differences in the expression levels of M1-like and M2-like macrophage markers in CNV lesions. We observed lower mRNA levels of markers for M2-like macrophages (type 1 arginase [Arg-1], Fizz1, Ym1/2, matrix metalloproteinase 9 [MMP9], MMP12, interleukin [IL]-10, platelet-derived growth factor subunit B [PDGF-B], Wnt5a, Wnt7b, IL-4, and IL-13) in kinase-dead RIP1$^{K45A/K45A}$ compared with WT and no significant difference in the mRNA levels of markers for M1-like macrophages (inducible nitric oxide synthase [iNOS], TNF, IL-6, IL-18, IL-23a, Cxcl1, Cxcl2, Cxcl10, and Cxcl11) (Fig. 5*A*). We also assessed the protein levels of VEGF and IL-12 using ELISA. VEGF-A is a marker for proangiogenic M2-like macrophages, whereas IL-12 is a marker of M1-like macrophages and a well-established antiangiogenic cytokine (41–43). We found that VEGF-A protein levels were down-regulated, whereas IL-12 protein levels were up-regulated in eyes with CNV lesions from RIP1$^{K45A/K45A}$ mice compared with those from WT mice (Fig. 5*B*). These data suggest that RIP1 kinase inhibition may not only up-regulate caspase-mediated cell death in macrophages but may also modulate M1/M2 polarization. Consistent with this impression, phosphorylation and activation of signal transducer and activator of transcription 1 (STAT1), a key transcription factor for M1 macrophages, was up-regulated in CNV lesions of RIP1$^{K45A/K45A}$ compared with WT, whereas phosphorylation and activation of STAT6, a key transcription factor for M2 macrophages, was suppressed (Fig. 5*C*). In addition, immunohistochemistry revealed down-regulation of M2 marker CD206 expression in the CNV macrophages of RIP1$^{K45A/K45A}$ mice (Fig. 5*D*).

Inhibition of RIP1 Kinase Activity Suppresses M2 Polarization of Macrophages in Vitro. The in vivo results suggested that catalytic inhibition of RIP1 has an additional nonapoptotic function that modulates macrophage activation by altering M1/M2 polarization. To further evaluate this, we used bone marrow-derived macrophages (BMDMs) in vitro and employed IL-4 to induce M2 phenotype. After 24 h, the RIP1 kinase inhibitor Nec-1 was added to the culture medium to levels not affecting viability (44, 45) (*SI Appendix*, Fig. S9) in order to assess cell death-independent

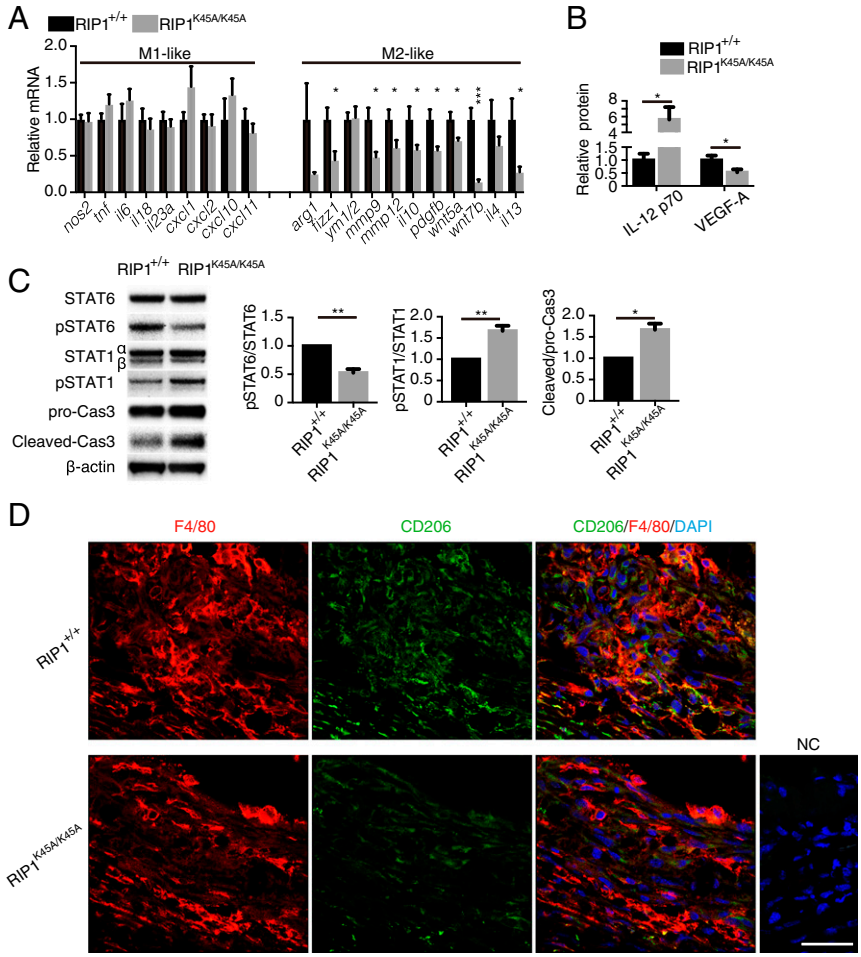

Fig. 5. (*A*) Relative mRNA levels on day 4 after CNV induction in RPE-choroid samples of RIP1$^{+/+}$ and RIP1$^{K45A/K45A}$ mice. $n = 6$ eyes per group. (*B*) Relative protein levels on day 5 after CNV induction in RPE-choroid samples of WT and RIP1$^{K45A/K45A}$ mice. $n = 6$ eyes per group for IL-12; $n = 14$ per group for VEGF-A. (*C*) Western blot analysis of STAT6, phospho-STAT6 (Tyr641), STAT1, phospho-STAT1 (Tyr701), procaspase-3, and cleaved caspase-3 in RPE-choroid on day 4 after CNV induction in RIP1$^{+/+}$ (left lane) and RIP1$^{K45A/K45A}$ mice (right lane). $n = 3$ samples per group. (*D*) Immunohistochemistry of day 4 CNV sections for CD206 and its localization in F4/80(+) macrophages in RIP1$^{+/+}$ and RIP1$^{K45A/K45A}$ mice. NC, negative control. (Scale bar, 50 μm.) $^{*}P < 0.05$, $^{**}P < 0.01$, $^{***}P < 0.001$; ns, no significant difference; Student's *t* test or 1-way ANOVA and post hoc Tukey's test. Data are mean ± SEM.

roles of RIP1 in M2 macrophages. Inhibition of RIP1 kinase by Nec-1 in IL-4–treated BMDMs resulted in caspase-8 activation and suppression of the critical M2 transcription factor STAT6 (Fig. 6*A*). Both effects were reversed by the pan-caspase inhibitor Z-VAD (Fig. 6*A*). A flow cytometry analysis of IL-4–induced M2 markers CD206(+) and CD163(+) showed significant reduction after RIP1 kinase inhibition, which was reversed by Z-VAD (Fig. 6*B*). Likewise, RIP1 kinase inhibition reduced production of M2 cytokine IL-10, and increased secreted M1 cytokine IL-1β, both of which were reversed by Z-VAD (Fig. 6*C*). Finally, we assessed the mRNA levels of M1/M2 macrophage polarization markers. After 24-h treatment with Nec-1, mRNA levels of M2 markers (Arg-1, Fizz1, and Ym1/2) were significantly down-regulated, and this effect was reversed by Z-VAD (Fig. 6*D*). With extended treatment using Nec-1 for 48 h, we observed significant up-regulation of mRNA levels of M1 markers (iNOS, IL-6, IL-23a, Cxcl1, Cxcl2, il12a, and Cxcl11), which was also abolished by Z-VAD treatment (Fig. 6*D*). These data support the notion that catalytic inhibition of RIP1 suppresses M2 polarization and may shift macrophages to M1 polarization, at least partially through caspase pathway activation. In addition, to rule out off-target effects of Nec-1 on macrophage polarization, BMDMs from RIP1 kinase-inactive $RIP1^{K45A/K45A}$ mice were used to confirm that genetic RIP1 kinase inhibition also suppresses M2 and enhances M1 marker mRNA expression (*SI Appendix*, Fig. S10).

Catalytic Inhibition of RIP1 Does Not Affect the Angiogenic Response in Endothelial Cells. RIP1 expression is considered ubiquitous, and RIP1 could be expressed at lower levels in vascular endothelial cells, suggesting that they may also play a role in mediating the effects of RIP kinase inhibition on angiogenesis. To assess this possibility, we examined the effects of Nec-1 treatment in vitro using cultured human umbilical vein endothelial cells (HUVECs). RIP1 kinase inhibition did not decrease the proliferation of HUVECs for up to 3.5 d of culture compared with vehicle (*SI Appendix*, Fig. S11*A*). In addition, RIP1 kinase inhibition did not affect the migration

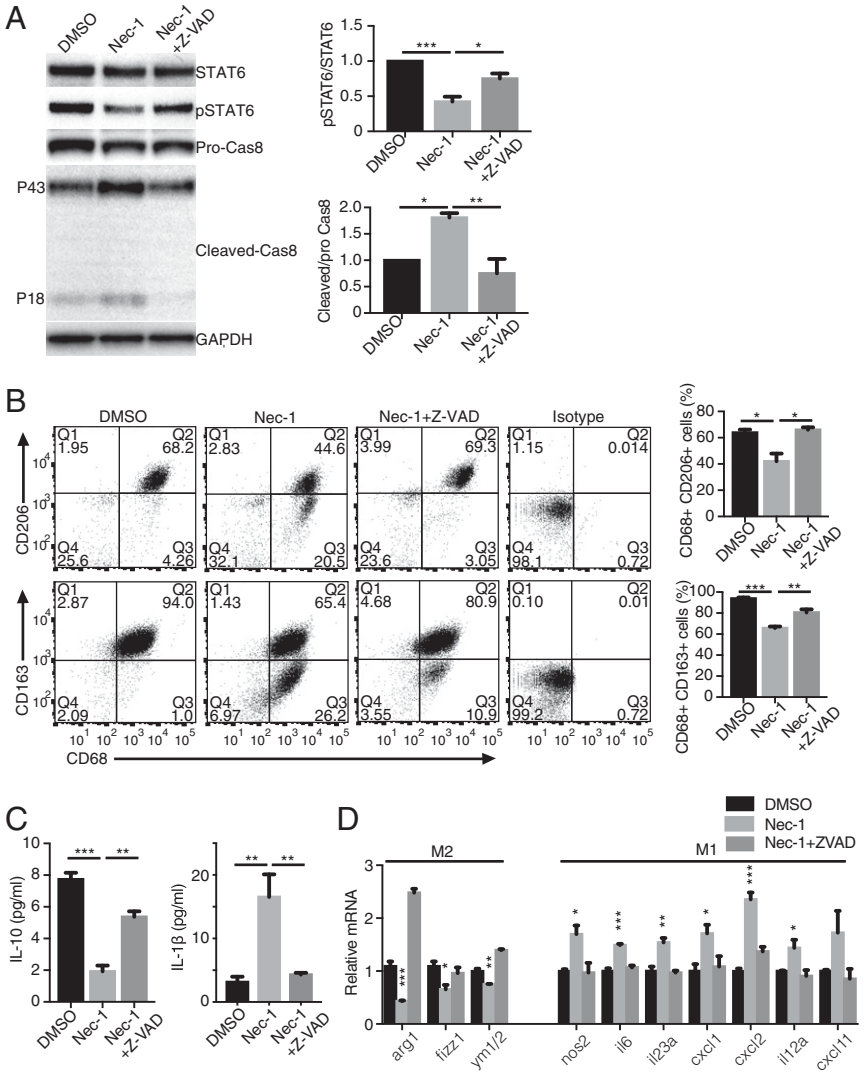

Fig. 6. Nec-1 suppresses M2 polarization of BMDMs in vitro through caspase activation. (*A*) Western blot analysis of STAT6, phospho-STAT6 (Tyr641), pro-caspase-8, and cleaved caspase-8 in M2-polarized BMDMs by IL-4 and treated with DMSO vehicle, Nec-1 (30 μM), or Nec-1 (30 μM) + Z-VAD (30 μM) for 48 h. $n = 3$ samples per group. (*B*) Flow cytometry analysis of M2-polarized BMDMs treated with Nec-1 (30 μM) or Nec-1 (30 μM) + Z-VAD (30 μM) for 48 h. Cells were stained for CD68, CD206, and CD163. $n = 3$ samples per group. (*C*) IL-10 and IL-1β secretion in supernatant by M2-polarized BMDMs treated with Nec-1 (30 μM) or Nec-1 (30 μM) + Z-VAD (30 μM) for 48 h. $n = 5$ samples per group. (*D*) Relative mRNA levels of M2-polarized BMDMs treated with Nec-1 (30 μM) or Nec-1 (30 μM) + Z-VAD (30 μM) for 24 h (for M2 markers) and 48 h (for M1 markers). $n = 3$ or 4 samples per group. $^*P < 0.05$, $^{**}P < 0.01$, $^{***}P < 0.001$; 1-way ANOVA and post hoc Tukey's (*A*–*C*) or Dunnett's test (*D*). Data are mean ± SEM.

of HUVECs tested using the scratch-wound assay (*SI Appendix*, Fig. S11*B*) or the tube-formation assay (*SI Appendix*, Fig. S11*C*).

Furthermore, we evaluated ex vivo choroidal angiogenesis by culturing 1 × 1-mm pieces of peripheral RPE-choroid-sclera on Matrigel using a procedure described previously (46–48). This system enables the assessment of choroidal angiogenesis without significant numbers of infiltrating macrophages. Consistent with the results on HUVECs, Nec-1 treatment did not suppress choroidal angiogenesis ex vivo (*SI Appendix*, Fig. S11*D*). Taken together, these results suggest that endothelial cells are not the direct target of catalytic inhibition of RIP1 to attenuate angiogenesis.

Discussion

RIP kinases have been extensively studied as key effectors of regulated cell death (necroptosis), and their role has been reported in many disorders, including neurodegenerative diseases (49–52), ischemic injuries (53), inflammatory diseases (54), and cancer metastasis (55). However, previous studies have not investigated the role of RIP kinases in vascular disorders. The present study demonstrates a nonnecrotic role for RIP1 kinase activity in angiogenesis. We showed that pharmacological and genetic inhibition of RIP1 kinase activity is effective in inhibiting angiogenesis in multiple in vivo models. Mechanistically, this effect is not mediated by RIP kinase inhibition in endothelial cells but appears to be mediated, at least partially, via RIP kinase inhibition-mediated caspase activation through the ripoptosome-like complex and suppression of M2 infiltrating macrophages. In contrast, caspase inhibition, which leads to activation of the necroptotic pathway (19–21), aggravates CNV in vivo (*SI Appendix*, Fig. S12*A*) and enhances M2 marker expression in BMDMs in vitro (*SI Appendix*, Fig. S12*B*). A schematic layout shown in Fig. 7 shows the balance between apoptotic and necroptotic pathways in macrophages that may dictate pathological angiogenesis.

Recent studies have unveiled new levels of complexity in cell-fate regulation by RIP1. For example, although RIP1 can activate RIP3, it also acts as a negative regulator of spontaneous RIP3 activation and necroptosis (23). Other experiments have revealed an essential function of RIP1 in preventing inappropriate activation of both caspase-8–dependent apoptosis and RIP3-dependent necroptosis in multiple tissues, including skin, liver, and intestine (24–26). In addition, RIP1 kinase-dependent apoptosis has also been observed in TNF-induced cell death, in which phosphorylation of the intermediate domain of RIP1 (Ser321 for mouse and Ser320 for human RIP1) controls RIP1 kinase-dependent apoptosis and necroptosis (56, 57). Overall, accumulating data have revealed multiple roles for RIP1 in determining cellular fate, depending on cell type and context; nevertheless, a complete understanding of this phenomenon remains elusive. Similar to RIP1, the role of RIP3 varies depending on the biological milieu. In addition to the necroptotic pathway induced by kinase-dependent RIP3 activity, a recent study revealed that genetic ($RIP3^{D161N/D161N}$) or pharmacological inhibition of RIP3 kinase leads to apoptosis via assembly of the ripoptosome-like complex harboring kinase-independent RIP1/RIP3, FADD, and caspase-8 (28, 29). These findings, as well as previous reports of Nec-1–induced apoptosis (30, 31), suggest a reciprocal regulation between apoptosis and necroptosis, in which caspase-8 blocks necroptosis through RIP1 cleavage, and RIP1/RIP3 kinase activity blocks apoptosis through an unknown mechanism (58). Kinase-inactive $RIP3^{D161N/D161N}$ knockin mice die during embryogenesis through increased apoptosis due to the scaffold function of RIP3, while kinase-inactive $RIP3^{K51A/K51A}$ mice are viable, likely from the substantially reduced expression of RIP3 (20). In addition, kinase-independent RIP3 function has also been proposed to control cytokine production in mononuclear phagocytes in the lamina propria of the intestine after treatment with dextran sodium sulfate (59).

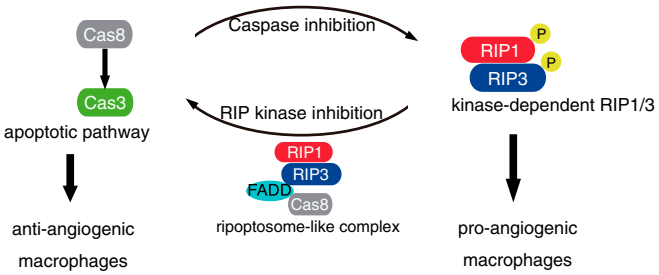

Fig. 7. Schematic summary for the present study. In angiogenesis-associated macrophages, Nec-1 treatment or kinase-inactive RIP1 activates caspases through the kinase-independent ripoptosome-like complex and suppresses M2 activation, thereby inhibiting angiogenesis. In contrast, caspase inhibition that augments RIP kinase activation aggravates pathological angiogenesis.

In the present study, RIP up-regulation was observed in lesions with new vessel formation, and RIP kinase inhibition suppressed angiogenesis formation. Because RIP1 is ubiquitously expressed, we sought to examine the cell type important for the observed phenomenon. Experiments in isolated cultured endothelial cells and in vascular explants without immune cells showed that RIP1 kinase inhibition did not affect vascular endothelial cell proliferation, tube formation, or vascular sprouting (*SI Appendix*, Fig. S11), suggesting that endothelial cells are not the critical cells in RIP1 kinase-regulated angiogenesis. Thus, we next turned our attention to the immune cells. Indeed, we found that when macrophages were depleted using clodronate, RIP1 inhibition by Nec-1 could not suppress neovascularization. Furthermore, adoptive transfer of WT macrophages to $RIP1^{K45A/K45A}$ mice reversed the suppression of neovascularization that was observed in $RIP1^{K45A/K45A}$ mice. These results suggest that macrophages play an important role in RIP1 kinase-mediated angiogenesis.

But how does RIP kinase inhibition in macrophages suppress angiogenesis? Since RIP kinases are essential in necroptotic cell death, we first examined this proposition. Although catalytic inhibition of RIP1 or RIP3 (Nec-1, GSK′872, or kinase-dead $RIP1^{K45A/K45A}$) suppresses angiogenesis, total deletion of RIP3 does not, suggesting that the inhibitory effect on angiogenesis is not mediated by inhibition of the necroptotic pathway alone. Previous reports have suggested that kinase inhibition of RIP3 unmasks a kinase-independent function of RIP3 that leads to activation of caspase-8 (28, 29). Similarly, studies have reported caspase-dependent apoptosis induced by Nec-1 treatment and inhibition of RIP1 kinase (30, 31). Based on this knowledge, we speculated that caspase activation by kinase-independent RIP function [which was unmasked by RIP kinase inhibition (28, 29)] contributes to the attenuation of angiogenesis. Indeed, we observed increased caspase activation in macrophages in CNV of Nec-1–treated eyes, and caspase inhibition by Z-VAD clearly blocked the inhibitory effect of Nec-1 on angiogenesis in laser-induced CNV, Matrigel plugs, and alkali injury-induced corneal neovascularization in mice. Furthermore, we observed an increased number of TUNEL(+) macrophages and caspase-3 activation by RIP1 kinase inhibition in CNV, and these effects were blocked by Z-VAD, suggesting that the apoptotic function of caspase was induced by RIP1 kinase inhibition in macrophages. Although induction of apoptotic cell death in macrophages could partially account for the suppression of angiogenesis [as it is known that macrophage depletion reduces angiogenesis (60, 61)], the number of TUNEL(+) cells in CNV lesions was relatively small. Thus, apoptotic function of caspase by itself in macrophages may not be able to satisfactorily explain the angiogenesis suppression observed. Therefore, we looked for other non–cell-death effects of RIP1 kinase inhibition and caspase activation in macrophage function. Since M2 macrophages are considered proangiogenic, we investigated the effect of RIP1 kinase

inhibition and caspase activity in macrophage M1/M2 polarization. Indeed, after RIP1 kinase inhibition, we observed down-regulation of M2-like and up-regulation of M1-like markers in macrophages. These effects of RIP1 kinase inhibition on M1/M2 polarization were reversed by the pan-caspase inhibitor Z-VAD, suggesting that caspase activation by RIP1 kinase inhibition leads to the suppression of M2 angiogenic macrophage phenotype in vivo. This was further corroborated by in vitro studies with BMDMs.

Previous work has shown that caspase-8 is not only an initiator of apoptotic cell death but also plays a nonapoptotic role in facilitating monocyte–macrophage differentiation (62–64). In addition, a previous study has shown that the caspase inhibitor IETD-CHO promotes M2 macrophage polarization in vitro, which is in line with our hypothesis (Fig. 7) (65). Another recent study also reported a vital role of caspase-8 in M1 polarization. In caspase-8–deficient macrophages, the RIP1/RIP3 necroptotic pathway was hyperactivated, which prevented normal M1 polarization (66). In contrast to these previous studies revealing a role of caspase in M1 polarization, the current study elucidates a role of RIP kinases in promoting M2 polarization through cell death-independent functions. During the submission process, a new study reported the role of RIP1 in facilitating M2 polarization in tumor-associated macrophages (67), which is consistent with our conclusion. In addition, our study showed that mechanistically, changes in M2 polarization after RIP kinase inhibition are associated with ripoptosome-like complex formation and caspase activation mediated by the scaffold properties of RIP kinases. Hence, our current study suggests an association between caspases and necroptotic pathways in controlling M1/M2 macrophage polarization.

We used multiple in vivo models of angiogenesis (laser CNV, corneal alkali injury, and Matrigel plug) and revealed similar nonnecrotic roles of RIP kinases in angiogenesis. However, other mechanisms may be critical in different angiogenic models and further studies would be welcome. For example, some researchers have suggested that spontaneously occurring vascular leakage and retinochoroidal anastomotic neovascularization in certain mouse strains might be useful to study (68), although the phenotype mimics a relatively uncommon human neovascular AMD that is called retinal angiomatous proliferation.

RIP kinase inhibitors have been considered candidates for the treatment of neurodegenerative disorders, including retinal degenerative disorders and dry AMD (69–72), diseases that can be complicated by additional pathological neovascularization. The current study suggests that RIP kinase inhibition does not induce neovascularization but rather suppresses it. This is important because other proposed candidates for treatment of dry AMD, such as inhibitors of complement component 3 (C3), led to increased rate of new neovascular AMD seen in human phase II clinical trials (73). Thus far, laser-induced CNV has been a rather robust model for the development of neovascular AMD treatments, and a reliability study using this model had predicted the proangiogenic effect of C3 inhibition, when carefully conducted in the most commonly used C57BL6/J mouse strain (74).

In summary, we have identified a previously unsuspected role for RIP1 kinase activity in angiogenesis that is mediated, at least partially, through nonnecrotic and nonapoptotic actions on macrophages. This work provides evidence for the potential therapeutic value of catalytic inhibition of RIP1 in attenuating angiogenesis through a macrophage-specific caspase activation mechanism. Furthermore, these findings shed light on the regulation of macrophage polarization and angiogenesis through the balance between RIP kinases and caspase activity.

Materials and Methods

Animal procedures were approved by the Animal Care Committee of Massachusetts Eye and Ear, and performed in accordance with the Association for Research in Vision and Ophthalmology Statement for the Use of Animals in Ophthalmic and Vision Research. RIP1$^{K45A/K45A}$ mice were kindly provided by GlaxoSmithKline. Rip3$^{-/-}$ mice and C57BL/6J mice were purchased from The Jackson Laboratory. These animals were backcrossed to C57BL/6J mice to remove the Crb1$^{rd8/rd8}$ mutation.

Detailed descriptions of the laser-induced CNV model, immunohistochemistry, Western blot, in vivo Matrigel plug assay, TUNEL staining, quantitative real-time RT-PCR, ELISA, HUVEC assays, ex vivo choroidal sprouting assay, BMDM culture, and flow cytometry can be found in *SI Appendix, Materials and Methods*.

ACKNOWLEDGMENTS. This work was supported by the Yeatts Family Foundation (D.G.V.); Monte J. Wallace (D.G.V.); 2013 Macula Society Research Grant Award (to D.G.V.); a Physician Scientist Award (to D.G.V.); unrestricted grant from the Research to Prevent Blindness Foundation (to J.W.M. and D.G.V.); National Eye Institute (NEI) R21EY023079-01/A1 (to D.G.V.); NEI Grant EY014104 (Massachusetts Eye and Ear Infirmary Core Grant) (to D.G.V.); Loeffler Family Fund (D.G.V.); R01EY025362-01 (to D.G.V.); ARI Young Investigator Award (to D.G.V.); Foundation Lions Eye Research Fund (D.G.V.); NIH NEI Core Grant P30EY003790 (to D.G.V.); Agence National de la Recherche; ERA-Net for Research on Rare Diseases, Institut Universitaire de France (D.G.V.); and a fellowship from the TOYOBO Biotechnology Research Foundation (to T.U.). We also thank Fengyang Lei for technical input.

1. L. S. Lim, P. Mitchell, J. M. Seddon, F. G. Holz, T. Y. Wong, Age-related macular degeneration. *Lancet* **379**, 1728–1738 (2012).
2. T. Lawrence, G. Natoli, Transcriptional regulation of macrophage polarization: Enabling diversity with identity. *Nat. Rev. Immunol.* **11**, 750–761 (2011).
3. J. Kelly, A. Ali Khan, J. Yin, T. A. Ferguson, R. S. Apte, Senescence regulates macrophage activation and angiogenic fate at sites of tissue injury in mice. *J. Clin. Invest.* **117**, 3421–3426 (2007).
4. N. Jetten *et al*., Anti-inflammatory M2, but not pro-inflammatory M1 macrophages promote angiogenesis in vivo. *Angiogenesis* **17**, 109–118 (2014).
5. R. Nakamura *et al*., IL10-driven STAT3 signalling in senescent macrophages promotes pathological eye angiogenesis. *Nat. Commun.* **6**, 7847 (2015).
6. S. Zandi *et al*., ROCK-isoform-specific polarization of macrophages associated with age-related macular degeneration. *Cell Rep.* **10**, 1173–1186 (2015).
7. K. L. Spiller *et al*., Sequential delivery of immunomodulatory cytokines to facilitate the M1-to-M2 transition of macrophages and enhance vascularization of bone scaffolds. *Biomaterials* **37**, 194–207 (2015).
8. Y. Yang *et al*., Macrophage polarization in experimental and clinical choroidal neovascularization. *Sci. Rep.* **6**, 30933 (2016).
9. L. Biancone *et al*., Development of inflammatory angiogenesis by local stimulation of Fas in vivo. *J. Exp. Med.* **186**, 147–152 (1997).
10. K. B. Nguyen, S. He, S. J. Ryan, P. Lopez, D. R. Hinton, Apoptosis in surgically excised subretinal neovascular membranes in age-related macular degeneration. *Invest. Ophthalmol. Vis. Sci.* **37**, 203–209 (1996).
11. X. Shi *et al*., Inhibition of TNF-alpha reduces laser-induced choroidal neovascularization. *Exp. Eye Res.* **83**, 1325–1334 (2006).
12. B. A. Di Bartolo *et al*., Tumor necrosis factor-related apoptosis-inducing ligand (TRAIL) promotes angiogenesis and ischemia-induced neovascularization via NADPH oxidase 4 (NOX4) and nitric oxide-dependent mechanisms. *J. Am. Heart Assoc.* **4**, e002527 (2015).
13. B. Fernández-Vega *et al*., Blockade of tumor necrosis factor-alpha: A role for adalimumab in neovascular age-related macular degeneration refractory to anti-angiogenesis therapy? *Case Rep. Ophthalmol.* **7**, 154–162 (2016).
14. K. Grote *et al*., Toll-like receptor 2/6 stimulation promotes angiogenesis via GM-CSF as a potential strategy for immune defense and tissue regeneration. *Blood* **115**, 2543–2552 (2010).
15. Q. Lin *et al*., High-mobility group box-1 mediates Toll-like receptor 4-dependent angiogenesis. *Arterioscler. Thromb. Vasc. Biol.* **31**, 1024–1032 (2011).
16. T. Fujimoto *et al*., Choroidal neovascularization enhanced by *Chlamydia pneumoniae* via Toll-like receptor 2 in the retinal pigment epithelium. *Invest. Ophthalmol. Vis. Sci.* **51**, 4694–4702 (2010).
17. L. Wu *et al*., Intravitreal tumor necrosis factor-alpha inhibitors for neovascular age-related macular degeneration suboptimally responsive to antivascular endothelial growth factor agents: A pilot study from the Pan American Collaborative Retina Study Group. *J. Ocul. Pharmacol. Ther.* **29**, 366–371 (2013).
18. N. M. Wagner, L. Bierhansl, G. Nöldge-Schomburg, B. Vollmar, J. P. Roesner, Toll-like receptor 2-blocking antibodies promote angiogenesis and induce ERK1/2 and AKT signaling via CXCR4 in endothelial cells. *Arterioscler. Thromb. Vasc. Biol.* **33**, 1943–1951 (2013).
19. J. Silke, J. A. Rickard, M. Gerlic, The diverse role of RIP kinases in necroptosis and inflammation. *Nat. Immunol.* **16**, 689–697 (2015).
20. K. W. Wegner, D. Saleh, A. Degterev, Complex pathologic roles of RIPK1 and RIPK3: Moving beyond necroptosis. *Trends Pharmacol. Sci.* **38**, 202–225 (2017).
21. D. Ofengeim, J. Yuan, Regulation of RIP1 kinase signalling at the crossroads of inflammation and cell death. *Nat. Rev. Mol. Cell Biol.* **14**, 727–736 (2013).

22. N. Festjens, T. Vanden Berghe, S. Cornelis, P. Vandenabeele, RIP1, a kinase on the crossroads of a cell's decision to live or die. *Cell Death Differ.* **14**, 400–410 (2007).
23. S. Orozco *et al*., RIPK1 both positively and negatively regulates RIPK3 oligomerization and necroptosis. *Cell Death Differ.* **21**, 1511–1521 (2014).
24. W. J. Kaiser *et al*., RIP1 suppresses innate immune necrotic as well as apoptotic cell death during mammalian parturition. *Proc. Natl. Acad. Sci. U.S.A.* **111**, 7753–7758 (2014).
25. M. Dannappel *et al*., RIPK1 maintains epithelial homeostasis by inhibiting apoptosis and necroptosis. *Nature* **513**, 90–94 (2014).
26. J. E. Roderick *et al*., Hematopoietic RIPK1 deficiency results in bone marrow failure caused by apoptosis and RIPK3-mediated necroptosis. *Proc. Natl. Acad. Sci. U.S.A.* **111**, 14436–14441 (2014).
27. V. Lambert *et al*., Laser-induced choroidal neovascularization model to study age-related macular degeneration in mice. *Nat. Protoc.* **8**, 2197–2211 (2013).
28. P. Mandal *et al*., RIP3 induces apoptosis independent of pronecrotic kinase activity. *Mol. Cell* **56**, 481–495 (2014).
29. K. Newton *et al*., Activity of protein kinase RIPK3 determines whether cells die by necroptosis or apoptosis. *Science* **343**, 1357–1360 (2014).
30. H. Jie *et al*., Necrostatin-1 enhances the resolution of inflammation by specifically inducing neutrophil apoptosis. *Oncotarget* **7**, 19367–19381 (2016).
31. W. Han, J. Xie, L. Li, Z. Liu, X. Hu, Necrostatin-1 reverts shikonin-induced necroptosis to apoptosis. *Apoptosis* **14**, 674–686 (2009).
32. S. P. Cartland, S. W. Genner, A. Zahoor, M. M. Kavurma, Comparative evaluation of TRAIL, FGF-2 and VEGF-A-induced angiogenesis in vitro and in vivo. *Int. J. Mol. Sci.* **17**, E2025 (2016).
33. J. H. Chang, E. E. Gabison, T. Kato, D. T. Azar, Corneal neovascularization. *Curr. Opin. Ophthalmol.* **12**, 242–249 (2001).
34. L. D. Ormerod, M. B. Abelson, K. R. Kenyon, Standard models of corneal injury using alkali-immersed filter discs. *Invest. Ophthalmol. Vis. Sci.* **30**, 2148–2153 (1989).
35. C. H. Dohlman *et al*., Chemical burns of the eye: The role of retinal injury and new therapeutic possibilities. *Cornea* **37**, 248–251 (2018).
36. F. Cade *et al*., Alkali burn to the eye: Protection using TNF-α inhibition. *Cornea* **33**, 382–389 (2014).
37. W. Stevenson, S. F. Cheng, M. H. Dastjerdi, G. Ferrari, R. Dana, Corneal neovascularization and the utility of topical VEGF inhibition: Ranibizumab (Lucentis) vs bevacizumab (Avastin). *Ocul. Surf.* **10**, 67–83 (2012).
38. H. S. Dua, A. J. King, A. Joseph, A new classification of ocular surface burns. *Br. J. Ophthalmol.* **85**, 1379–1383 (2001).
39. M. J. Roper-Hall, Thermal and chemical burns. *Trans. Ophthalmol. Soc. U. K.* **85**, 631–653 (1965).
40. S. B. Berger *et al*., Cutting edge: RIP1 kinase activity is dispensable for normal development but is a key regulator of inflammation in SHARPIN-deficient mice. *J. Immunol.* **192**, 5476–5480 (2014).
41. C. Sgadari, A. L. Angiolillo, G. Tosato, Inhibition of angiogenesis by interleukin-12 is mediated by the interferon-inducible protein 10. *Blood* **87**, 3877–3882 (1996).
42. M. Strasly *et al*., IL-12 inhibition of endothelial cell functions and angiogenesis depends on lymphocyte-endothelial cell cross-talk. *J. Immunol.* **166**, 3890–3899 (2001).
43. Y. Zhou *et al*., Interleukin-12 inhibits pathological neovascularization in mouse model of oxygen-induced retinopathy. *Sci. Rep.* **6**, 28140 (2016).
44. J. Wu *et al*., Mlkl knockout mice demonstrate the indispensable role of Mlkl in necroptosis. *Cell Res.* **23**, 994–1006 (2013).
45. B. Lamothe, Y. Lai, M. Xie, M. D. Schneider, B. G. Darnay, TAK1 is essential for osteoclast differentiation and is an important modulator of cell death by apoptosis and necroptosis. *Mol. Cell. Biol.* **33**, 582–595 (2013).
46. Z. Shao *et al*., Choroid sprouting assay: An ex vivo model of microvascular angiogenesis. *PLoS One* **8**, e69552 (2013).
47. R. S. Sulaiman *et al*., A novel small molecule ameliorates ocular neovascularisation and synergises with anti-VEGF therapy. *Sci. Rep.* **6**, 25509 (2016).
48. H. D. Basavarajappa *et al*., Ferrochelatase is a therapeutic target for ocular neovascularization. *EMBO Mol. Med.* **9**, 786–801 (2017).
49. G. Trichonas *et al*., Receptor interacting protein kinases mediate retinal detachment-induced photoreceptor necrosis and compensate for inhibition of apoptosis. *Proc. Natl. Acad. Sci. U.S.A.* **107**, 21695–21700 (2010).
50. Y. Murakami *et al*., Receptor interacting protein kinase mediates necrotic cone but not rod cell death in a mouse model of inherited degeneration. *Proc. Natl. Acad. Sci. U.S.A.* **109**, 14598–14603 (2012).
51. Y. Ito *et al*., RIPK1 mediates axonal degeneration by promoting inflammation and necroptosis in ALS. *Science* **353**, 603–608 (2016).
52. K. Sato *et al*., Receptor interacting protein kinase-mediated necrosis contributes to cone and rod photoreceptor degeneration in the retina lacking interphotoreceptor retinoid-binding protein. *J. Neurosci.* **33**, 17458–17468 (2013).
53. D. M. Rosenbaum *et al*., Necroptosis, a novel form of caspase-independent cell death, contributes to neuronal damage in a retinal ischemia-reperfusion injury model. *J. Neurosci. Res.* **88**, 1569–1576 (2010).
54. L. Duprez *et al*., RIP kinase-dependent necrosis drives lethal systemic inflammatory response syndrome. *Immunity* **35**, 908–918 (2011).
55. B. Strilic *et al*., Tumour-cell-induced endothelial cell necroptosis via death receptor 6 promotes metastasis. *Nature* **536**, 215–218 (2016).
56. M. B. Menon *et al*., $p38^{MAPK}$/MK2-dependent phosphorylation controls cytotoxic RIPK1 signalling in inflammation and infection. *Nat. Cell Biol.* **19**, 1248–1259 (2017).
57. I. Jaco *et al*., MK2 phosphorylates RIPK1 to prevent TNF-induced cell death. *Mol. Cell* **66**, 698–710.e5 (2017).
58. S. R. Mihaly, J. Ninomiya-Tsuji, S. Morioka, TAK1 control of cell death. *Cell Death Differ.* **21**, 1667–1676 (2014).
59. K. Moriwaki, S. Balaji, J. Bertin, P. J. Gough, F. K. M. Chan, Distinct kinase-independent role of RIPK3 in $CD11c^+$ mononuclear phagocytes in cytokine-induced tissue repair. *Cell Rep.* **18**, 2441–2451 (2017).
60. E. Sakurai, A. Anand, B. K. Ambati, N. van Rooijen, J. Ambati, Macrophage depletion inhibits experimental choroidal neovascularization. *Invest. Ophthalmol. Vis. Sci.* **44**, 3578–3585 (2003).
61. D. G. Espinosa-Heidmann *et al*., Macrophage depletion diminishes lesion size and severity in experimental choroidal neovascularization. *Invest. Ophthalmol. Vis. Sci.* **44**, 3586–3592 (2003).
62. T. B. Kang *et al*., Caspase-8 serves both apoptotic and nonapoptotic roles. *J. Immunol.* **173**, 2976–2984 (2004).
63. C. Rébé *et al*., Caspase-8 prevents sustained activation of NF-kappaB in monocytes undergoing macrophagic differentiation. *Blood* **109**, 1442–1450 (2007).
64. S. P. Cullen, S. J. Martin, Caspase activation pathways: Some recent progress. *Cell Death Differ.* **16**, 935–938 (2009).
65. H. Roca *et al*., CCL2 and interleukin-6 promote survival of human $CD11b^+$ peripheral blood mononuclear cells and induce M2-type macrophage polarization. *J. Biol. Chem.* **284**, 34342–34354 (2009).
66. C. M. Cuda *et al*., Conditional deletion of caspase-8 in macrophages alters macrophage activation in a RIPK-dependent manner. *Arthritis Res. Ther.* **17**, 291 (2015).
67. W. Wang *et al*., RIP1 kinase drives macrophage-mediated adaptive immune tolerance in pancreatic cancer. *Cancer Cell* **34**, 757–774.e7 (2018).
68. F. Qiu *et al*., Therapeutic effects of PPARα agonist on ocular neovascularization in models recapitulating neovascular age-related macular degeneration. *Invest. Ophthalmol. Vis. Sci.* **58**, 5065–5075 (2017).
69. Y. Murakami *et al*., Programmed necrosis, not apoptosis, is a key mediator of cell loss and DAMP-mediated inflammation in dsRNA-induced retinal degeneration. *Cell Death Differ.* **21**, 270–277 (2014).
70. Y. Murakami, J. W. Miller, D. G. Vavvas, RIP kinase-mediated necrosis as an alternative mechanisms of photoreceptor death. *Oncotarget* **2**, 497–509 (2011).
71. A. Al-Moujahed *et al*., Receptor interacting protein kinase 3 (RIP3) regulates iPSCs generation through modulating cell cycle progression genes. *Stem Cell Res.* **35**, 101387 (2019).
72. J. W. Miller, S. Bagheri, D. G. Vavvas, Advances in age-related macular degeneration understanding and therapy. *US Ophthalmic Rev.* **10**, 119–130 (2017).
73. D. S. Liao *et al*., Complement C3 inhibitor pegcetacoplan for geographic atrophy secondary to age-related macular degeneration: A randomized phase 2 trial. *Ophthalmology*, 10.1016/j.ophtha.2019.07.011 (16 July 2019).
74. S. H. Poor *et al*., Reliability of the mouse model of choroidal neovascularization induced by laser photocoagulation. *Invest. Ophthalmol. Vis. Sci.* **55**, 6525–6534 (2014).